FLUID STRUCTURE INTERACTION DESIGN DEVELOPMENT OF PASSIVE ADAPTIVE COMPOSITE INTERNATIONAL MOTH FOIL

L. Marimon Giovannetti, University of Southampton, UK, Laura.Marimon-Giovannetti@soton.ac.uk
J. Banks, University of Southampton, UK, J.Banks@soton.ac.uk
M. Ledri, Land Rover BAR, UK, matteo.ledri@gmail.com
S.W. Boyd, University of Southampton, UK, S.W.Boyd@soton.ac.uk
S.R. Turnock, University of Southampton, UK, S.R.Turnock@soton.ac.uk

The International Moth is a single-handed ultra-lightweight foiling development class boat, and it follows open class rules. Therefore, the designer and builder have full liberty to develop and produce the fastest boat [1]. It is possible to adapt the internal structure of the fixed foil to achieve a tailored twist angle for a given load. Exploring the possibility of using Passive Adaptive Composite (PAC) on the moth hydrofoil to control its pitch angle enables the boat to achieve a stable flight in a wide range of weather conditions whilst reducing the induced drag, passively decreasing the angle of attack in increased boat speed. Using PAC in a multi-element foil, such as the International Moth one, will allow the structure to achieve a constant lift force with speeds higher than the design take-off speed with less need to constantly modifying the rear foil section. Toward the development of a PAC moth fixed foil, experimental and numerical results for a single element aerofoil, able to achieve a linear decrease in lift coefficient with increase in wind speed, are presented and discussed. The results present the aero-elastic response of the foil explaining the complexity involved in fluid-structure interaction problems.

NOMENCLATURE

Symbol	Definition	[unit]
A_{ij}	In-plane stiffness [**A**]	
AoA	Angle of Attack	[deg]
B_{ij}	Bending-extension coupling [**B**]	
CFD	Computational Fluid Dynamics	
C_L	Lift coefficient	
D_{ij}	Bending stiffness [**D**]	
DIC	Digital Image Correlation	
DSBT	Dirrential Stiffness Bend-Twist	
FEA	Finite Element Analysis	
FSI	Fluid Structure Interaction	
k	Number of layer	
$k_{x,y,xy}$	Laminate curvature	
M_{ij}	Moments per unit length	[Nm]
N_{ij}	Forces	[N]
PAC	Passive Adaptive Composites	
PIV	Particle Image Velocimetry	
Q_{ij}	Stiffness matrix components	
t	Layer thickness	[mm]
V_S	Wind speed	[ms^{-1}]
W	Weight	[kg]
y^+	y-plus value	
z	Layer distance from the ref. plane	[mm]
α	Angle of attack	[deg]
γ_{xy}	Shear strain	
Δt	Exposure time PIV camera	[μs]
ϵ	Strain	
σ	Stress	[MPa]
τ_{xy}	Shear stress	[MPa]

1 INTRODUCTION

Among the sailing community there were developments on rig-tension gauges in the past twenty years in order to achieve accurate and repeatable tuning guides for static load on rigging. Cable tension gauges generally operate using the same principle, bending the cable between three points and measuring the reactive force on one of those points either mechanically with a spring or electronically with a strain gauge [2]. With the recent increase of foiling boats there is still a lack of accurate measures of structural response and shape of the foils. This gives rise to scientific questions on whether there is a manufacturing consistency between the port and starboard foil on a catamaran or different batches of foils on mono-hulls. The aim of the current research is therefore to develop an experimental methodology capable of accurately describing the structural response of a full-scale foil under fluid-load and to design and develop a foil structure tailored to decrease its lift coefficient by mean of increased flow speed.

The experimental technique used to measure foil deformations is Digital Image Correlation (DIC). DIC has been used at

a variety of scales from high magnification [3], to large-scale structures [4] and has previously been used to measure foil deflections under fluid loads, with a technique developed at the University of Southampton [5,6]. This technique involves the use of digital cameras that register a series of images of a surface onto which a randomised speckle pattern is applied. The key advantages are the use of simple equipment (i.e. cameras, lenses, light and computer), the fact that is a non-contact measurement and its high fidelity of precision [7]. Within the DIC software, the correlation between speckle pattern in subsequent images is used to determine how the structure has deformed in time, thereby allowing the derivation of the full-field deflections and strains of the investigated object [8]. The use of two cameras, in a stereo configuration, allows for the measurement of deformations both in the plane normal to the camera and out-of-plane.

Measuring the deformation and twist of a foil under known static load allows the assessment of its bending and torsional stiffness [9]. Once the structural properties of the foil are known, it is possible to understand the effects of bending and twisting of the foil on the overall sailing performances. For the International Moth, shown in Figure 1, the change in lift coefficient with angle of attack for a Vendor T-foil was presented in [10].

Figure 1: *Forces acting on an International Moth whilst sailing.*

Having investigated the tip deflection and twist in characteristic sailing loads during a laboratory test, as described in [9], it was possible to assess that the tip deflection reduces the component of lift in the vertical direction as each end of the T-foil curves upward. Furthermore, the twist deformation associated with a downstream shift in centre of pressure (i.e. a 8% chord distance between the shear centre and the centre of pressure), reduces the local angle of attack by 0.23 degrees resulting in a 5% decrease in the generated lift force. Therefore it is clear that even under steady sailing loads the foil structural characteristics for a quasi-isotropic composite will have a noticeable effect on the performances of the boat.

The current paper will initially describe two techniques that can be used to change the performance profile of an International Moth foil. Moreover, the experimental and numerical results for a single element aerofoil, able to achieve a linear decrease in lift coefficient with increased wind speed, will be discussed.

2 BACKGROUND ON BEND-TWIST COUPLING

In developing the design of a single-element foil that can twist toward feather with increased flow-speed, two bent-twist techniques are brought together: the bend-twist coupling due to the orientation of the plies utilising Passive Adaptive Composites and the bend-twist coupling due to stiffness variation along the aerofoil chord utilising Differential Stiffness Bend-Twist (DSBT).

- PAC presents fibres oriented in the same direction at opposite sides of the neutral axis, introducing an interaction between the hydrodynamic forces and the laminate curvatures and between the hydrodynamic moments and the laminate strains. Wind turbine blade design and adaptivity were initially investigated during the 70_s and 80_s as a way to alleviate tip loads during wind gusts. Using the anisotropy of the material, it is possible to design components presenting elastic couplings that will enhance the performance of the whole structure [11, 12]. In those structures, the relationship of the stresses and strains must take into consideration the complete stiffness matrix as the stresses (σ and τ) and strains (ϵ and γ) are coupled to σ_1 and/or σ_2 in the two principal directions, leading to:

$$\begin{bmatrix} \sigma_x \\ \sigma_y \\ \tau_{xy} \end{bmatrix} = \begin{bmatrix} \bar{Q}_{11} & \bar{Q}_{12} & \bar{Q}_{16} \\ \bar{Q}_{12} & \bar{Q}_{22} & \bar{Q}_{26} \\ \bar{Q}_{16} & \bar{Q}_{26} & \bar{Q}_{66} \end{bmatrix} \begin{bmatrix} \epsilon_x \\ \epsilon_y \\ \gamma_{xy} \end{bmatrix} \quad (1)$$

where $\mathbf{Q_{ij}}$ represents the stiffness matrix in principal axis. Changing the ply angle in each lamina influences the stiffness matrix $\mathbf{Q}$ as the material axis is not aligned with the laminate axis. Under fluid loading, the forces and moments experienced by the composite will be related to the strains at laminate level as:

$$\begin{bmatrix} N_x \\ N_y \\ N_{xy} \\ M_x \\ M_y \\ M_{xy} \end{bmatrix} = \begin{bmatrix} \mathbf{A} & \mathbf{B} \\ \mathbf{B} & \mathbf{D} \end{bmatrix} \begin{bmatrix} \epsilon_x \\ \epsilon_y \\ \gamma_{xy} \\ k_x \\ k_y \\ k_{xy} \end{bmatrix} \quad (2)$$

where N_x, N_y, N_{xy} are the fluid forces, M_x, M_y, M_{xy} are the fluid moments, k_x, k_y, k_{xy} are the laminate cur-

vatures and

$$A_{ij} = \sum_{k=1}^{N} (\bar{Q}_{ij})_k t_k;\ i,j = 1,2,6 \qquad (3)$$

represents the in-plane stiffness of the laminate (and presents values also for symmetric and balanced layups)

$$B_{ij} = \sum_{k=1}^{N} (\bar{Q}_{ij})_k t_k \bar{z}_k;\ i,j = 1,2,6 \qquad (4)$$

represents the bending and/or extension coupling (i.e. the coupling term between moments and direct strains and forces and curvatures) and

$$D_{ij} = \sum_{k=1}^{N} (\bar{Q}_{ij})_k \left(t_k \bar{z}_k^2 + \frac{t_k^3}{12} \right);\ i,j = 1,2,6 \qquad (5)$$

represents the bending stiffness of the component. In equations (3-5) k is the layer number and t_k is the thickness of the k^{th} layer. In equations (4-5) $\bar{z}_k$ is the distance from the mid-plane to the centroid of the k^{th} layer. In order to correctly design Passive Adaptive Composites, it is necessary to account for the $\mathbf{B_{ij}}$ matrix as it gives the coupling terms for the bending-twist and extension-twist from the fluid-loads to the laminate structure. The $\mathbf{B_{ij}}$ matrix for symmetric and balanced laminate structures is zero as there are no coupling terms between moments and direct strains. The bend-twist coupling is deriving from plies oriented at the same angle at each side of the neutral axis. The oriented plies allow to achieve tailored designs for an expected load, inducing a twist on the hydrofoil section.

- DSBT has been introduced initially in [13] with a conceptual investigation of a beam-like structure and its response to flexural load with different web-stiffness. By stiffening one side of the web more than the other, it is possible to induce twist to the structure. This concept is particularly important in hydrofoil structures and their hydro-elastic behaviour. Indeed, by stiffening the leading edge of a foil, the shear centre is moved forward, away from the centre of pressure, resulting in a structure twisting toward feather under bending load.

  Changing the stiffness along the aerofoil chord to modify the shear centre position with respect to the centre of pressure is further analysed in [14] as a way of load alleviation in wind turbine blades.

Investigating the literature available to date on both techniques is important, during the development of the new foil-design, to understand the influence of both stiffness and passive adaptivity on the changes in effective angle of attack.

3 OPTIMISED DESIGN FOR BEND-TWIST COUPLING

Conventional foil performances assume a rigid shape, therefore the lift and drag coefficients are measured in experimental and numerical simulations for rigid sections. However, once analysing composite flexible foils, it is important to understand the effects of deflections on performance outcome. The International Moth horizontal foil provides the lift necessary to counteract the crew-hull weight, as presented in Figure 1. The produced force is dependant on the pitch angle as well as the boat speed squared. It is formed of a fixed and a moving elevator, as shown in Figure 2. In current foil design, both the fixed foil and elevator are made of quasi-isotropic composite material and the lift coefficient is controlled constantly changing the flap angle, and therefore section shape, with the bow-wand to maintain a constant lift force for different boat speeds.

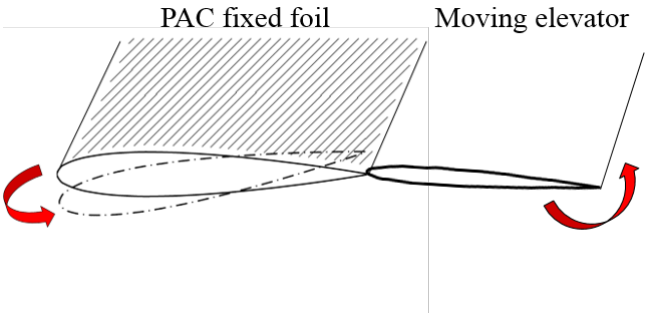

Figure 2: *Passive Adaptive Composite main foil associated with moving elevator. In increased boat speeds the main element would twist toward feather and the elevator would reduce the total camber of the foil, following the red arrows.*

An ideal lift profile aims to achieve a constant level of lift at a chosen take-off speed, Figure 3.

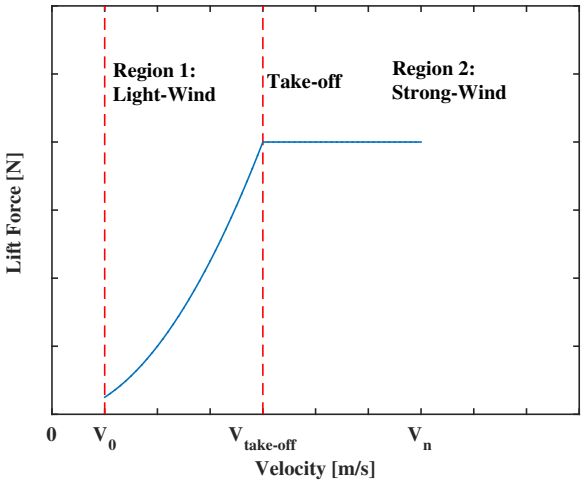

Figure 3: *Ideal lift over velocity profile for a hydrofoil section.*

In order to achieve a constant lift-curve, not only should the angle of attack change substantially but also the shape of the aerofoil, so as to decrease C_L linearly over V^2. The blue arrow in Figure 4 represents a way in which the hydrofoil could achieve a constant lift value, combining a PAC foil with a rear elevator to change the shape of the overall foil at different wind speeds. Figure 4 shows two typical lift coefficient curves

for a cambered and a symmetric section. Using passive adaptivity it is possible to change the angle of attack, decreasing the C_L value with increasing speed. This leads to a linear variation of lift with velocity, however, passive adaptive coupling requires an increase in tip deflection, and therefore lift force, to achieve a change in angle of attack. Therefore, bend-twist coupling is not able to achieve a constant lift force alone and the change in shape given by the rear flap is still needed. Decreasing the lift coefficient with speed at high angles of attack allows the delay of the stall angle, twisting the aerofoil toward feather. The ability to reduce the lift coefficient with increased flow speed allows to reduce also the induced drag, as the induced drag decreases proportionally to a decrease in angle of attack. Presenting a PAC main foil leads to less movements of the flap element, therefore leading to a reduction of skin friction, associated with the change in shape. For a hydrofoil design the effectiveness of passive adaptivity at low angles of attack (pitch angles) is important, as the rake has a limited range of angles adjustments. The current research proposes to understand the influences of building a PAC fixed foil that can twist toward feather in high boat speeds (i.e. when large tip deflections are occurring) to decrease the induced drag reducing the inflow angle.

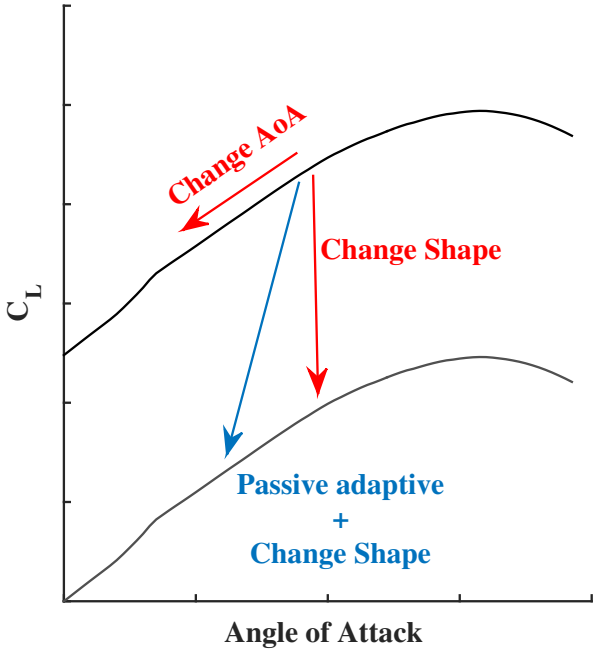

Figure 4: *Lift coefficient curves for cambered and symmetric sections. The arrows show the influence of using PAC composites that change the angle of attack, and the change in section shape that can be achieved with multi-elements foils or flaps.*

The design development of a PAC main foil element that can subsequently be adapted to an International Moth fixed foil is herein described together with results from full-scale experimental and numerical tests.

In order to achieve a level of twist high enough to reduce the rate of change of lift with speed, it is necessary to maximise the distance between the shear centre and the centre of pressure, and that the PAC oriented plies should lie as far apart as possible from the neutral axis. When the bending and torsional stiffness are increased, a reduction in coupling effects is seen. This leads to the necessity to chose a C-beam internal stiffener which enables to use the benefits of both bend-twist coupling techniques described in section 2.

The section shape of a daggerboard tip from the America's cup team Land Rover Ben Ainslie Racing was assessed and the shape was compared to a NACA 2412, as can be seen from Figure 5.

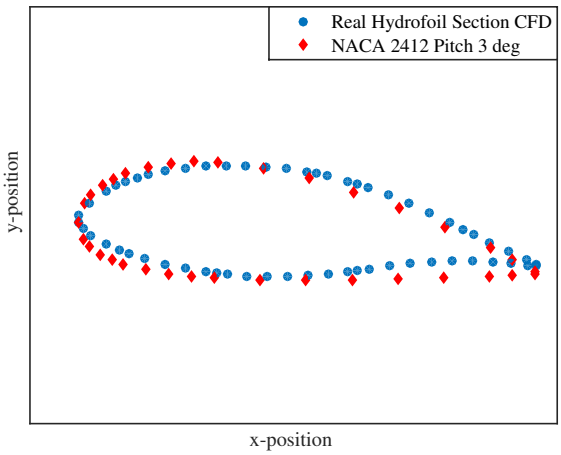

Figure 5: *Section shape of a real hydrofoil tip and of a NACA 2412 aerofoil.*

The NACA 2412 shape presents a very similar shape and camber to the daggerboard tip section. Therefore, in order to create a design that can be reproduced, the NACA section was chosen. It has to be noted that in order to reach the take-off speed in a foiling boat a pitch angle of $\approx 3^\circ$ is often set.

A large twist angle, induced by the internal C-spar being close to the leading edge of the foil and by the PAC oriented plies, could create inverse loading conditions during tests on a cambered aerofoil fixed at one end. An inverse loading condition would result in the failure of the structure as the cambered tip section would be loaded with an effective negative angle of attack. Therefore, an initial pre-twist is introduced along the span of the aerofoil. Furthermore, as the amount of twist increases from the root to the tip, a section shape with no-camber is chosen at the root (i.e. NACA0015) to create a small amount of lift in the root area. At half-span a NACA1412 section is introduced with a pre-twist angle of 1.5 degrees. This section shape is introduced to allow a smooth transition between a NACA0015 and a NACA2412, especially considering the glueing process of the Mylar sheet. Finally, at the tip, a NACA2412 is chosen with a pre-twist of 3 degrees, as presented in Figure 6.

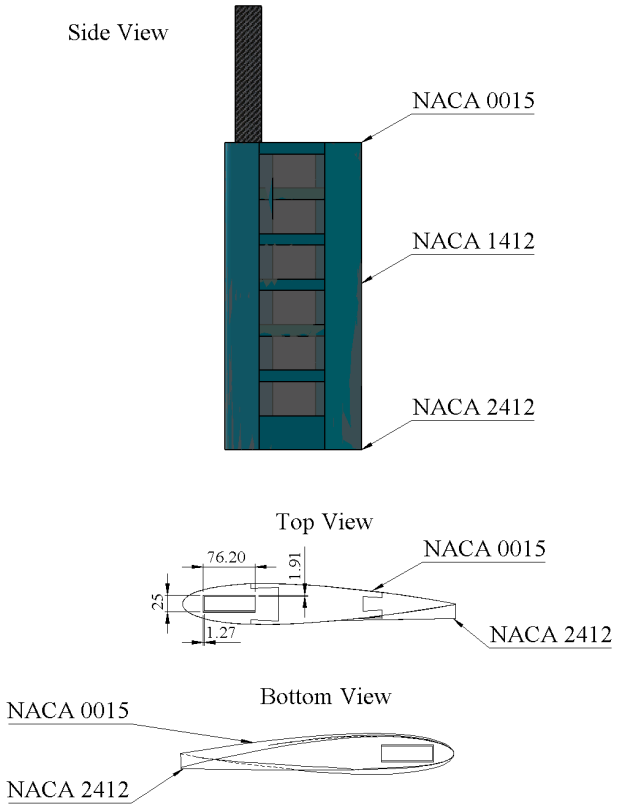

Figure 6: *Foil technical drawing showing the different section shapes and the principal dimensions. All the dimensions shown are in millimetres.*

4 NUMERICAL AND EXPERIMENTAL SET-UP

Given the high costs involved in experimental campaigns, it was necessary to achieve enough confidence in the response of the foil prior to entering the wind tunnel. Therefore, the numerical tools, validated against experimental values for an earlier design case, were used as design and developing tools to ensure a tailored response to load. The aerofoil shown in Figure 6 was modelled in the numerical environment. The structural model was solved using the numerical software ABAQUS 6.14, coupled to the fluid solver Star-CCM+ 11.0.2 through the Co-Simulation Engine (CSE). The C-beam was laminated with 4 plies as quasi-isotropic in the three surfaces [$\phi = 0/45/-45/0$] and two bend-twist coupling plies on the top and bottom surfaces [$\phi = 30/30$]. So the top surface laminate was modelled as [$\phi = 0/45/-45/0/30/30$] from bottom to top. The finite element model of the foil section closely represents the wind tunnel specimen, Figure 7(a). The material properties of the carbon, foam and Mylar were tested independently at the University of Southampton. The CFD environment was also set to replicate the wind tunnel experiments, representing the same dimensions of the working section of the wind tunnel in the y and z directions (i.e. width and height of the wind tunnel). For the CFD domain it was also important to represent correctly the boundary layer mesh, shown in Figure 7(b), and the transition along the span from the symmetric aerofoil section to the asymmetric one. The CFD mesh was approximately formed of 4.8 million cells and the FEA mesh of 50,000 elements.

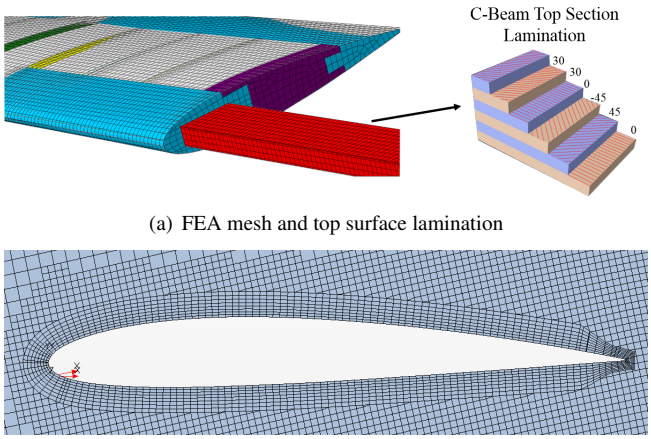

(a) FEA mesh and top surface lamination

(b) CFD tip section boundary layer mesh

Figure 7: *FSI numerical model mesh.*

The settings used for the fluid-structure interaction numerical model are summarised in Table 1.

Table 1: FSI numerical settings within Star-CCM+.

Simulation item	**Set-up**
Type of mesh	Trimmer Surface remesher Prism layer mesher
No. of elements	4.8 million
y^+ on aerofoil	>50
Boundary layer thickness	0.018 m
Turbulence intensity	0.002
Turbulent viscosity ratio	34
Domain physics	k-ω SST fully turbulent model γRe_θ transition model ABAQUS co-simulation
Solver	Implicit unsteady
Coupling step time	0.0025 s
Morpher solver	Morph from zero
Inlet	Velocity inlet
Outlet	Pressure outlet
Bottom and sides walls	Symmetry plane
Top wall	Wall free stream velocity
Aerofoil + beam	Wall no slip condition

The aerofoil was manufactured, built and tested at the University of Southampton. Two internal spars were produced to understand the influence of passive adaptivity in different materials. One C-beam was made only of pre-preg unidirectional carbon plies [15]: in top and bottom faces ϕ=[0/45/-45/0/30/30]$_C$. The second beam was manufactured

with pre-preg unidirectional quasi-isotropic E-Glass plies [16] and carbon PAC plies: in top and bottom faces ϕ=[0/45/-45/0]$_G$+[30/30]$_C$. During the manufacturing of the beams, the composite plies were layered, ensuring that the angle conventions were the same as the ones modelled numerically.

The structure was tested in the R. J. Mitchell closed circuit wind tunnel. The internal spar was fixed to the dynamometer via a Rexroth ® frame, as described in [5, 6].

For the tests on the foil, both DIC and PIV were high-speed systems. All four cameras and the laser were positioned in the viewing room, as can be seen in Figure 8. The same DIC set up used in [6] was used in the new experimental set-up. The high-speed stereo PIV equipment is detailed in Table 2.

Table 2: PIV performance table showing the equipment and the setting used.

Equipment	**Set-up**
Camera	2 Phantom v xx1 Sensor size: 25.6×16 mm Pixel size: 10 μm Resolution (max): 2560 × 1600 pixels Exposure time: 2498 μs Frame rate: 0.2-0.4 kHz Stereo angle: $\approx$ 39.5 deg. Δt= 60-40-30-25-20 μs for V_S= 10-15-20-25-30 m/s
Lens	Nikon 200 mm f4 Aperture: f-4 Depth of field: 16 mm
Laser	LD75-G PIV High repetition rate DPSS Nd:YAG Wavelength: 532 nm Output energy: 7.5 mJ at 10kHz

Figure 8(a) shows a schematic drawing of the equipment in the wind tunnel. The high-speed laser was positioned in the viewing room and the laser beam was deviated through two mirrors angled at 45° to obtain a focused sheet positioned 1/3 of chord downstream of the trailing edge. The PIV calibration was performed calibrating the left-had camera (Cam1) with the front of the calibration plate and the right-hand camera (Cam2) with the back of the calibration plate.

Having set the laser in the viewing room together with the DIC cameras, in order to ensure optical isolation between the two systems, it was necessary to apply a filter on the DIC cameras with transmittance of 0% in the green-wavelength region. The R-60 filter by [17] was installed on the DIC cameras. The LED lights were also covered with magenta gel filters to allow the high-speed DIC cameras to only detect two-thirds of the white light histogram, cutting off the laser wavelength. Moreover, two low-pass 532 nm ± 10 nm filters were applied to the PIV high-speed cameras to allow them to only capture the laser wavelength.

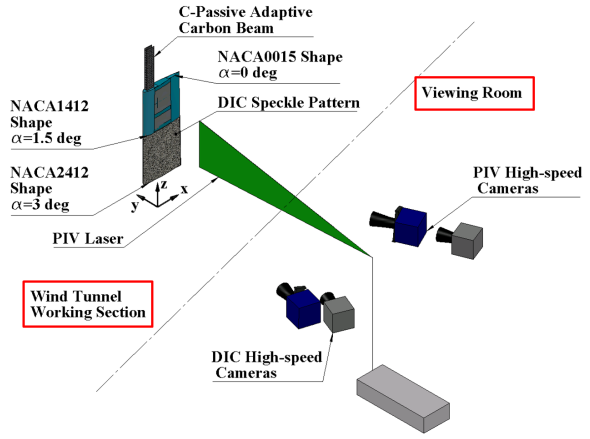

(a) Wind tunnel set up drawing

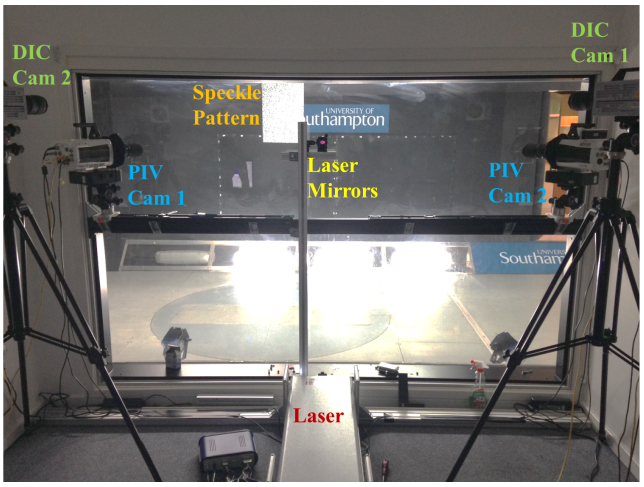

(b) Viewing room set-up

Figure 8: *Wind tunnel and equipment set-up.*

5 FSI RESULTS

Figure 9 presents the lift force response for $\alpha = 10.02°$ and a range of wind speeds. The two internal structures are compared. It is possible to see that the glass-carbon C-beam, being more flexible and prone to twist, allows a larger reduction in lift over velocity slope. This response is possible due to the larger bend-twist coupling effects occurring in the structure with less bending and torsional stiffness.

Both the numerical and wind tunnel data show that it is possible to design a structure tailored to a design goal controlling the level of bend-twist coupling. The presented results significantly reduce the increase in lift force with speed, ensuring that is possible to use numerical FSI methods to aid the design of tailored structures.

Designing for the inherent flexibility of a foil structure, it is possible to change the lift to velocity squared ratio.

The influence of both the deflection and the twist affect the aerodynamic response and vice-versa. For this reason it is important to understand and accurately measure the interactions between the flow features and the structure.

The lower torsional rigidity of the glass fibres leads to an in-

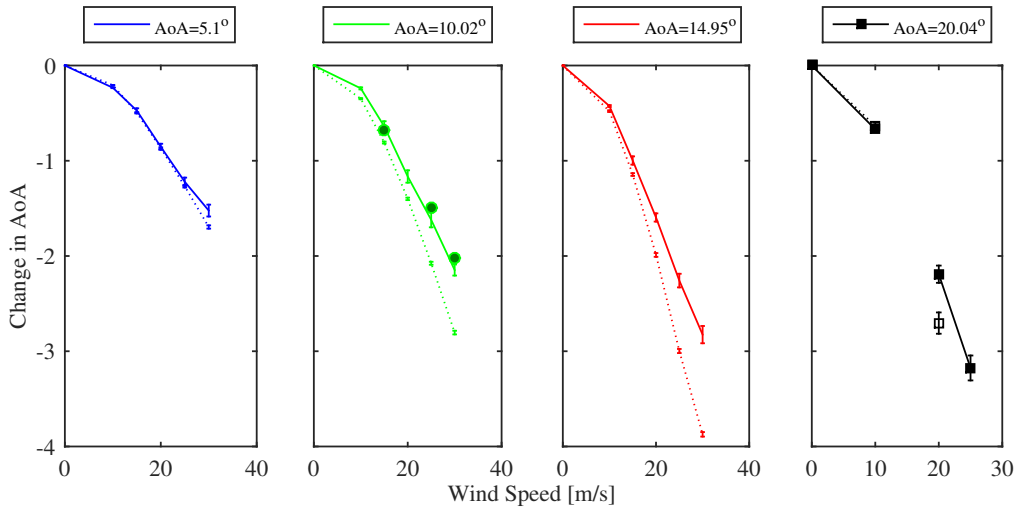

Figure 10: *Change in angle of attack for different wind speeds and set-angles of attack at 90% of aerofoil span. The solid lines represent the carbon spar and the dotted lines represent the glass-carbon spar as measured in the wind tunnel. For α=20.04° the closed marker indicates the carbon beam and the open marker the glass-carbon beam. The green markers presented for α=10.02° show the FSI twist for the modelled aerofoil with a carbon spar.*

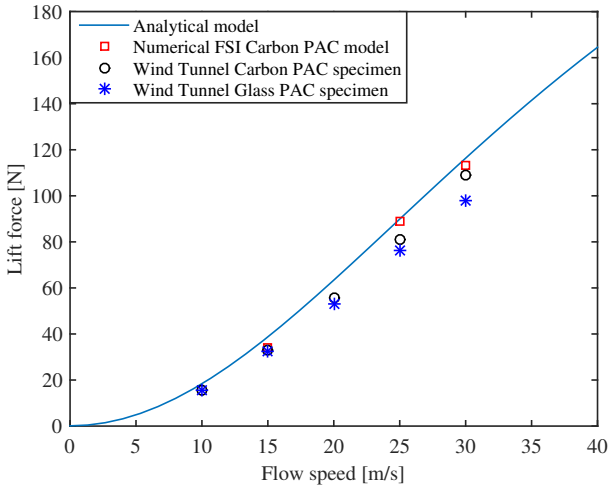

Figure 9: *Lift force over wind speed for $\alpha = 10.02°$: analytical, numerical FSI and wind tunnel results.*

crease in twist values (Figure 10). From both figures it is possible to see how the FSI numerical model correctly captures the twist and the aerodynamic response of the aerofoil with a carbon spar. The FSI numerical model present a slightly higher torsional stiffness (maximum twist error at $V_S = 25$ m/s of 7%) due to the discrepancies in the internal spar dimensions and the fillet of the C-spar edges manufactured to easily slide the spar in the foam leading edge. The possibility of achieving large changes in angle of attack even at the lowest set-angles of attack, enables to use a PAC foil for high-performance sailing boats. The foil can passively adjust its angle of attack to reduce the induced drag associated with the foiling configuration and the lift once reached the take-off speed.

6 CONCLUSIONS

The possibility of using Passive Adaptive Composites in the design of the fixed part of the International Moth foil has been presented. The advantages deriving from using bend-twist coupling techniques such as PAC and DSBT have been explained. Designing a foil for a high-performance boat taking into consideration the flexibility of the structure, changes the performance profile of the foil, leading to a decrease in induced drag and of lift force whist the foil passively reduces its angle of attack in increased boat speeds. Combining a fixed PAC foil with a movable elevator, enables to change not only the angle of attack but also the shape of the whole foil structure, leading to a plateau of lift force after the design take-off speed. A fluid-structure interaction numerical model was used as a design development tool for a single-element aerofoil. An accurate experimental methodology was used to validate simulations and assess the structural behaviour of the aerofoil under wind load for two different internal structures. Both the numerical and experimental results show that is possible to design a structure tailored to a certain load. The increase in lift with velocity is significantly reduced compared to a rigid section. The glass/carbon-fibre C-beam, with a lower torsional and bending stiffness compared to the full-carbon one, can achieve changes in angles of attack of almost 4 degrees for V_S = 25m/s and α = 14.95°. The results from the numerical simulations and experimental tests show the complexity of the interactions between a fluid and a structure and the importance of capturing the deflections and twists of foils when analysing their performances. The single-element aerofoil presented will be the base for the design of a new foil for the International Moth.

7 ACKNOWLEDGEMENTS

The authors would like to acknowledge the EPSRC for funding this research under the grant number EP/I009876/1. The authors would also thank the University of Southampton, the members of the TSRL and Dave Marshall and his team in the R. J. Mitchell wind tunnel. Moreover, we would like to thank Dr Nila from LaVision for his assistance with the DIC and PIV set-up.

REFERENCES

[1] International Moth Class, "International Moth Class Rules," tech. rep., 2013.

[2] S. Ltd, "Rig-Sense," tech. rep., 2015.

[3] G. Crammond, S. Boyd, and J. Dulieu-Barton, "Speckle pattern quality assessment for digital image correlation," *Optics and Lasers in Engineering*, vol. 51, pp. 1368–1378, Dec. 2013.

[4] N. Mccormick, "Digital image correlation for structural measurements," *Proceedings of the Institution of Civil Engineers*, vol. 165, pp. 185–190, 2012.

[5] J. Banks, L. Marimon Giovannetti, X. Soubeyran, A. Wright, S. R. Turnock, and S. W. Boyd, "Assessment of Digital Image Correlation as a method of obtaining deformations of a structure under fluid load," *Journal of Fluids and Structures*, vol. 58, pp. 173–187, 2015.

[6] L. Marimon Giovannetti, J. Banks, S. R. Turnock, and S. W. Boyd, "Uncertainty assessment of coupled Digital Image Correlation and Particle Image Velocimetry during wind tunnel experiments," *Journal of Fluids and Structures*, vol. 68, pp. 125–140, 2017.

[7] Z. Tang, J. Liang, Z. Xiao, and C. Guo, "Large deformation measurement scheme for 3D digital image correlation method," *Optics and Lasers in Engineering*, vol. 50, pp. 122–130, Feb. 2012.

[8] P. Rastogi and E. Hack, *Optical Methods for Solid Mechanics: A Full-Field Approach*. 2012.

[9] J. Banks, L. Marimon Giovannetti, J. Taylor, and S. R. Turnock, "Assessing Human-Fluid-Structure Interaction for the International Moth," *Procedia Engineering*, vol. 147, pp. 311–316, 2016.

[10] B. Beaver and J. Zseleczky, "Full scale measurement on a hydrofoil International Moth," in *19th Cheasap. Sail. YACHT Symp.*, 2009.

[11] V. Fedorov, *Bend-Twist Coupling Effects in Wind Turbine Blades*. PhD thesis, Technical University of Denmark, 2012.

[12] P. Veers, S. N. Laboratories, G. Bir, N. Renewable, N. Wind, and D. Lobitz, "Aeroelastic Tailoring in Wind-Turbine Blade Applications," *Wind Energy*, 1998.

[13] W. Raither, A. Bergamini, and P. Ermanni, "Profile beams with adaptive bending-twist coupling by adjustable shear centre location," *Journal of Intelligent Material Systems and Structures*, vol. 24, pp. 334–346, 2012.

[14] M. T. Herath, A. K. L. Lee, and B. Gangadhara Prusty, "Design of shape-adaptive wind turbine blades using Differential Stiffness Bend-Twist coupling," *Ocean Engineering*, vol. 95, pp. 157–165, 2015.

[15] Gurit, "SE 84 LV Low temperature cure epoxy prepreg," tech. rep., 2012.

[16] PRF Composite Materials, "Toughened Epoxy Prepreg System RP-528: low-medium temperature cure 85-120 deg C," tech. rep., 2015.

[17] Edmund Optics, 2016.

8 AUTHORS BIOGRAPHY

L. Marimon Giovannetti is currently a research fellow for the Sport Performance Laboratory in the Fluid Structure Interaction group at the University of Southampton and a sailor campaigning for the 2020 Olympics in Tokyo in the NACRA 17 class. She successfully defended her PhD thesis in January 2017 with a thesis entitled: "Fluid structure interaction testing, modelling and development of Passive Adaptive Composite foils". During her PhD she has been working as an intern in the design team of Land Rover BAR from November 2015 until April 2017.

J. Banks is a New Frontiers Fellow working in experimental and computational fluid dynamics. His research focuses on assessing the hydrodynamic performance of deforming structures such as flexible foils, ships and human based systems. He is involved in various projects for the Performance Sport Engineering Laboratory working with the English Institute of Sport. His interest in the use of engineering tools for high-performance sport application started during his PhD where he developed experimental coaching tools for British Swimming in the build up to the London 2012 Olympic games.

M. Ledri obtained his MSc degree in Naval Architecture and Marine Engineering at the University of Trieste in 2004. He's been involved in the America's Cup for the last two editions, first with Artemis Racing and now with Land Rover BAR, where he is part of the design team and works on CFD, FSI and performance analysis. He's also involved in other projects regarding high performance yachts and superyachts.

S. W. Boyd is an Associate Professor at the University of Southampton with background in Naval Architecture. His research activities concentrate mainly on the application of polymer composites in the maritime environment and sailing industry. Stephen investigates both the barriers to the use of composite materials and potential avenues for exploitation of their favourable properties in hydrofoil design.

S. R. Turnock is Professor of Maritime Fluid Dynamics as well as Director of Performance Sports Engineering Lab at the University of Southampton. His expertise is in the

synthesis of experimental, computational and theoretical fluid dynamics analysis to improve performance. He has a long standing interest in foil performance having studied propeller-rudder interaction for his PhD.